HHS Public Access

Author manuscript

J Neurosci Methods. Author manuscript; available in PMC 2021 April 15.

Published in final edited form as:

J Neurosci Methods. 2020 April 15; 336: 108631. doi:10.1016/j.jneumeth.2020.108631.

An emerging method to noninvasively measure and identify vagal response markers to enable bioelectronic control of gastroparesis symptoms with gastric electrical stimulation

Matthew P. Ward[1,2], **Anita Gupta**[2], **John M. Wo**[2], **Bartek Rajwa**[3], **John B. Furness**[4,5], **Terry L. Powley**[1,6], **Thomas V. Nowak**[2]

[1]Weldon School of Biomedical Engineering, Purdue University, West Lafayette, IN, USA

[2]Indiana University School of Medicine, Indianapolis, IN, USA

[3]Bindley Bioscience Center, Purdue University, West Lafayette, IN, USA

[4]Department of Anatomy and Neuroscience, University of Melbourne, Parkville, Australia

[5]Florey Institute of Neuroscience and Mental Health, Parkville, Australia

[6]Dept. of Psychological Sciences, Purdue University, West Lafayette, IN, USA

Abstract

Background: Gastric electrical stimulation (GES) can be a life-changing, device-based treatment option for drug-resistant nausea and vomiting associated with diabetic or idiopathic gastroparesis (GP). Despite over two decades of clinical use, the mechanism of action remains unclear. We hypothesize a vagal mechanism.

New Method: Here, we describe a noninvasive method to investigate vagal nerve involvement in GES therapy in 66 human subjects through the compound nerve action potential (CNAP).

Results: Of the 66 subjects, 28 had diabetic GP, 35 had idiopathic GP, and 3 had postsurgical GP. Stimulus charge per pulse did not predict treatment efficacy, but did predict a significant increase in total symptom score in type 1 diabetics as GES stimulus charge per pulse increased ($p < 0.01$), representing a notable side effect and providing a method to identify it. In contrast, the number of significant left and right vagal fiber responses that were recorded directly related to patient symptom improvement. Increased vagal responses correlated with significant decreases in total symptom score ($p < 0.05$).

Comparison with Existing Method(s): We have developed transcutaneous recording of cervical vagal activity that is synchronized with GES in conscious human subjects, along with

Competing Interest Statement

Dr. Ward has pending and granted patents pertaining to the use of evoked nerve responses as feedback signals for stimulus waveform optimization. This intellectual property is owned and managed by the Purdue Research Foundation and Office of Technology Commercialization. No other authors have a competing interest to declare.

methods of discriminating the activity of different nerve fiber groups with respect to conduction speed and treatment response.

Conclusions: Cutaneous vagal CNAP analysis is a useful technique to unmask relationships among GES parameters, vagal recruitment, efficacy and side-effect management. Our results suggest that CNAP-guided GES optimization will provide the most benefit to patients with idiopathic and type 1 diabetic gastroparesis.

Keywords

Gastroparesis; Gastric electrical stimulation; Vagus nerve; Compound nerve action potential; Neurostimulation; Bioelectronics

1. Introduction

1.1. History of gastroparesis and gastric electrical stimulation therapy

Gastroparesis (GP) is a chronic gastrointestinal disorder characterized by a delayed clearance of food from the stomach to the small intestine. The primary symptoms are nausea (~92%), vomiting (~84%), abdominal bloating (~75%) and early satiety (~60%) [1, 2]. A diagnosis is based on gastric emptying scintigraphy and the presence of one or more characteristic symptoms of gastroparesis for more than 3 months [3].

Gastric electrical stimulation (GES) of the stomach, including presumably local vagal branches, is an effective treatment for nausea and vomiting, though less effective in augmenting emptying, in gastroparetic patients who have been refractory to other forms of medical therapy. How GES relieves nausea and vomiting in symptomatic patients is unclear. Human studies of gastroparetic patients using PET scanning show that GES produces changes in blood flow to specific areas of the central nervous system. Experiments in anesthetized rodents show that GES of the antrum and stimulation of the cervical vagus nerve produce vagal compound nerve action potentials (CNAPs) that can be measured with implanted cuff electrodes and with Ag/AgCl disk electrodes positioned on the skin surface over the mid cervical vagal nerves [4].

Nearly six decades ago, Bilgutay *et al.* (1963) demonstrated the potential of GES of the antrum as a treatment for gastroparesis at the University of Minnesota Medical School. They reasoned that electrical stimulation might entrain gastrointestinal motility much like a cardiac pacemaker entrains the pumping action of the heart, because the gastrointestinal tract is lined with naturally occurring pacemaker cells along its length. Using the modified tip of a nasogastric tube, Bilgutay *et al.* stimulated the antral portion of the stomach in dogs. They observed stimulation-induced gastric contractions and a net increase in the rate of food clearance from the stomach [5]. Further studies showed that certain GES parameter combinations entrain the basal electrical activity of the stomach in humans and canines; optimal entrainment is achieved when stimulating at a slightly higher rate than the intrinsic electrical pacemaker activity of the stomach [6–9]. These observations led to clinical investigations that demonstrated improvements in nausea and vomiting symptoms using GES in human patients with gastroparesis [10, 11]. The Medtronic Enterra GES system is currently the only FDA-approved GES system in the United States, and is intended as a last-

resort option for patients with treatment-resistant nausea and vomiting due to idiopathic or diabetic gastroparesis.

1.2. Motivation and approach

Despite decades of research, the optimal GES parameters for treating the specific symptoms of gastroparesis remain unclear, as do the mechanisms behind their reported efficacy. There are two broad classes of stimulus parameters: High frequency, short-pulse stimuli, which are in clinical use, and low frequency, long-pulse stimuli, which are not in clinical use. Both are reported as effective for relieving symptoms of nausea and vomiting, but only the latter has been shown to entrain gastric electrical activity and promoting gastric motility [12]. Since clinical GES parameters are not effective for promoting motility and since the vagus is the primary nerve supply to the stomach, we hypothesize that GES modulates nausea and vomiting through a vagal mechanism. Due to the natural variation in disease etiology and GES electrode placement relative to gastric vagal afferent fibers [13], along with inherent anatomical and physiological differences, we further posit that each patient will likely require a unique, personalized set of stimulus parameters and electrode placements to engage specific vagal afferent pathways that mediate effective GES therapy, and some may never see a benefit.

Patients who have an implanted GES device undergo intermittent stimulation of the stomach wall through bipolar wire electrodes implanted along the greater curvature of the ventral stomach approximately 10 cm proximal to the pylorus (Fig. 1). Electrodes are always implanted in this manner and are always separated by 1 cm. The stimulus is delivered through the stimulating leads by an implantable pulse generator (IPG) that is placed subcutaneously in the abdominal region. These impulses are typically delivered with a stimulus pulse current of 5 to 10 mA, a stimulus pulse duration of 330 μs, a 14, 28, or 55 Hz pulse repetition frequency, a 0.1-2 s ON time, and a 3-5 s OFF time. The amplitude, frequency and pulse duration of these stimuli are typically varied over time according to a protocol provided by Medtronic to methodically identify a combination of parameters that patients report as beneficial. These settings can be changed with an external wand that is placed on the patient’s abdomen overlying the IPG. Since no physiological feedback signals are measured, the process can take months to complete and does not address individual symptom profiles or side effects.

The Gastroparesis Cardinal Symptom Index (GCSI) is a patient survey that clinicians use to gain a better understanding of the type and severity of symptoms experienced by patients with gastroparesis (e.g., postprandial fullness/early satiety, nausea/vomiting and bloating). Revicki *et al.* (2003) report an internal consistency reliability of 0.84, a test-re-rest reliability of 0.76, and congruency with clinician assessments [14]. The GCSI is often used to keep track of the efficacy of GES therapy at specific device settings. GES device settings are adjusted at regular intervals until the patient and clinician are satisfied or the device settings are maximized. By observing whether GCSI scores correlate with features of the vagal CNAP, we aim to establish a system through which the data can teach us how to stimulate the vagus nerve in order to achieve symptom resolution, which could in turn accelerate the development of feedback-controlled, personalized bioelectronics for gastroparesis and other

diseases with vagal involvement. To accomplish this in human subjects for whom there is not an option for invasive nerve recordings, we developed a protocol to collect noninvasive recordings of the GES-evoked vagal CNAP. If the signals detected from the skin surface over the vagal nerves is vagal, we expect that certain features of the signal will be present when patients report symptom resolution or symptom worsening (e.g., side effects of treatment).

1.3. Significance of approach

In this paper, we report an emerging new method to noninvasively resolve important features of the GES-evoked vagal compound nerve action potential (CNAP) responses in human subjects, using validated gastroparesis symptom survey data and traditional approaches to CNAP analysis to resolve associations between phase-locked CNAP responses to GES and patient symptom profiles. Using this tool for GES from the skin surface, we present data which strongly suggest that the GES-mediated recruitment of specific (presumably afferent) vagal nerve fiber populations, grouped by their conduction speed, predict symptom improvement. This new approach to measure and classify vagal responses with respect to symptom profiles provides:

1. A method to measure vagal nerve activation in a completely noninvasive manner, and confirm observed clinical outcomes
2. A data-driven path to develop a diagnostic test that determines if and how a patient might benefit from GES therapy (e.g., via temporary, endoscopically-placed or percutaneous GES electrodes that can be used to determine whether a patient might benefit from GES prior to undergoing surgery for a permanent implant) [15]
3. A data-driven approach to better manage symptoms in existing patients receiving GES therapy using the vagal response as feedback to titrate GES parameters
4. A data-driven approach to identify nerve response patterns that predict off-target effects from stimulation
5. A new set of tools to help other inform the design and functionality of bioelectronic interventions for gastroparesis and other indications.

2. Materials and Methods

2.1. Study context and overview

All clinical study procedures were performed at the Digestive and Liver Disorders (DALD) Center at the Indiana University School of Medicine (Indianapolis, IN) under an IRB-approved Human Subjects Research protocol (IRB #: 1206008988). Gastroparesis patients who had undergone implantation of a GES device as treatment for refractory nausea and vomiting secondary to GP were considered candidates for study. Subjects were allowed to voluntarily enroll in the study regardless of their symptom history or perception of treatment efficacy using the GES device.

As a pure observational study, our design did not alter patient treatment in any way (i.e., we did not reprogram the device from the prescribed settings, we did not change any current

medication use, we did not change their diet, and we did not provide any expectation that the study or its outcome would provide any potential benefit to the patient). This observational study approach provided a unique neural response marker discovery platform through which study data could be screened for any potential associations between evoked responses measured from the electrodes placed on the skin surface over the left/right cervical vagus nerve and symptom profiles collected through a visual analog scale at the time of data collection. Importantly, the observational study design was expected to reduce or eliminate any possibility of a placebo effect, because we did not alter their treatment plans in any way. Fig. A.1 provides an overview of the data collection and analysis protocols. Each step is described in detail in the following sections of the Materials and Methods.

2.2. Noninvasive measurement of GES-evoked vagal CNAPs in human

2.2.1. GCSI survey and cutaneous electrode placement—Subjects were asked to complete the GCSI symptom survey after providing informed consent to enroll into the study (Fig. A.1; Step 1) [14]. The data collection expert, who was responsible for collecting all study data and maintaining confidentiality, interrogated the GES device of each subject prior to placing the cervical recording electrodes. This was done in order to identify and document the existing/prescribed stimulus parameters (Fig. A.1; Step 2), the impedance between the stimulating electrodes, and the output voltage setting of the device (the Enterra GES device sets the stimulus current by applying a voltage computed according to the measured resistance of the electrodes via Ohm's law). After instructing the subject to lay down on their back, the skin surface overlying the left and right cervical vagus nerve was cleaned with alcohol swabs and allowed to dry.

A pair of cutaneous recording electrodes (conventional Ag/AgCl gel pad electrodes that are used to collect electrocardiogram data) were placed on the skin surface of the neck overlying the left and right mid-cervical vagus nerve (Fig. A.1; Step 3), spaced ~3 cm apart within the carotid triangle, with the active electrode just medial to the border of the sternocleidomastoid and lateral to the laryngeal prominence, and the reference electrode ~3 cm superior to the active electrode along the medial border of the ipsilateral sternocleidomastoid (the area described is located slightly anterior to the sternocleidomastoid muscle, just inferior to the angle of the jaw and superior to its clavicular insertion). A large surface area common ground/reference electrode was placed on the xiphoid process or ipsilateral mastoid. To facilitate the recording process, a pea-sized drop of conductive electrolyte gel was applied to the center of each EKG electrode before placing it on the skin. After connecting the electrodes and prior to data acquisition, we estimated the distance that a nerve signal would be expected to travel before reaching the first recording electrode by measuring the distance between the surface position deduced to overlie the implanted GES electrodes and the distal left cervical recording electrode (i.e., the first cutaneous electrode that an afferent vagal signal would pass on its way from the stomach to the solitary nucleus). This critical measurement was necessary to standardize the classification of CNAP data collected from different subjects with different vagal nerve lengths. The conduction distance was always measured by the same investigator following the same procedure.

All data were collected with the ADInstruments PowerLab data acquisition system via their Octal BioAmp analog front end (Fig. A.1; Step 4) or their EOG pods. A Lead II electrocardiogram (EKG) was measured during acquisition, which was later conditioned (Section 2.2.2) and used to detect the GES-generated stimulus artefacts (and thus the timing of GES stimulation). Recordings were collected for 3-5 min at the patient's prescribed GES parameters, followed by 3-5 min of recording with the device off, and finally by 3-5 min of recording with the device turned back on again. All data were digitized at 10 kHz and de-identified prior to handing the raw recordings and conduction distance to Purdue for further processing and analysis (Fig. A.1; Step 5).

2.2.2. Extracting the mean response to GES from the cutaneous vagal recordings—Clinical study data were analyzed in single-blind fashion using custom analysis scripts written in Matlab R2015a. Analysis was performed on de-identified subject data with no prior knowledge of device settings, implant date, efficacy, or any other information beyond the location of the pad electrodes used to measure the data in Channels 1-3 of the ADInstruments PowerLab System and the conduction distance (Ch1: EKG; Ch2: Left cutaneous vagal electroneurogram; Ch3: Right cutaneous vagal ENG). Care was taken to standardize the method of analysis and data interpretation for each subject. Ensemble averaging was one method used to standardize the analysis (Fig. A.1; Step 6).

A stimulus artefact template for ensemble averaging was formed from the mean of six randomly selected segments of data in the high pass-filtered EKG channel (see below). In each case, the template started just before a stimulus artefact and ended just before the next stimulus artefact. If we assume the most common stimulus frequency setting of 14 Hz, then the artefact template can be no longer in duration than approximately 71 ms. Fig. 2B shows an example of the typical morphology of the stimulus artefact, in this case for a 55 Hz stimulus frequency having a period of approximately 18 ms.

We designed a custom event detection workflow in Matlab to locate, extract, align and average all segments of the measured data that match the shape and timing of the stimulus artefact template (where the stimulus artefacts have a sufficient presence for software-based detection, almost always only in the EKG trace). The location of each stimulus artefact was first detected in the EKG trace via the normalized cross-correlation (normxcorr2 function in Matlab) of the stimulus artefact template and a zero-phase, high pass-filtered replica of the EKG trace (f_c = 30 Hz; f_p = 50 Hz; a zero-phase, finite impulse response equiripple filter, designed to suppress the EKG signal, while preserving the shape and phase of the stimulus artefact with respect to the left and right cutaneous vagal recordings). The output of the normalized cross-correlation function was cubed to further distinguish the regions where the template and portions of the EKG signal matched versus regions where they did not match (the rate of attenuation increases faster for smaller values closer to 0 than the larger values closer to 1 when multiplied by themselves). The cubed cross-correlation function (CCF) output was then fed into a function that detected the temporal position of peaks in the CCF output signal whose amplitude was greater than 0.9 (or 90% of the maximum possible signal amplitude). We next used these time indices (i.e., the location of the start of each detected stimulus artefact in the file) to extract and average phase-locked response data from the left and right cutaneous vagal ENG recording channels. The number of stimulus-response

segments extracted from each file depended on the recording duration and pulse repetition frequency setting on the device of each patient.

2.2.3. Standardizing and classifying features of the mean GES-evoked response—The mean stimulus-response waveforms, computed from an average of hundreds of GES-evoked responses extracted from the left and right cutaneous recording traces (up to 600+ in cases of 28 or 55 Hz stimulation), were then plotted as a function of conduction velocity (i.e., conduction speed) to account for differences in conduction distance among the pool of patient data (a method to standardize the data for population-based analysis by reducing the influence of CNAP conduction time differences between subjects that could result simply from a difference in the distance that the evoked signal had to travel before passing the first recording electrode) (Fig. A.1; Step 7). Conduction velocity (i.e., speed) was computed by dividing the conduction distance, d_C (measured from the center of skin surface over the deduced stimulating electrode location to the distal recording electrode, in mm, as shown in Fig. 1), by the latency, t_C (in ms), of each sample relative to the start of a stimulus pulse. All subsequent analysis was performed in the conduction velocity domain in order to account for signal dispersion in the time domain that would prohibit the reliable identification of common features across subjects. The mean CNAP signal was then baseline-adjusted by subtracting the mean of all CNAP response samples from each CNAP response sample, which centered the signal around the 0 V line. The 95% confidence interval (1.96 times the standard error of the mean) about the mean CNAP response at successive sample was then computed (Fig. A.1; Step 8) in a similar manner (e.g., using each baseline-adjusted CNAP response detected from a subject) prior to the response classification step.

The baseline-adjusted, mean stimulus-response data (i.e., candidate CNAP) from the left and right vagal channels were next parsed by conduction velocity using the Letter System for nerve fiber classification [16]. Within the confines of the Letter System, mean CNAP response volleys from each subject were then classified in terms of I) showing a significant response (e.g., presence of an Aβ/Aγ response whose magnitude is significantly different from 0 V at $\alpha = 0.05$), II) not showing a response (e.g., no fiber response volleys are detected and/or the magnitude of the response volley is not significantly different from 0 V at $\alpha = 0.05$), or III) data are corrupted by noise, identified as high-amplitude, highly-periodic oscillations that match 60 Hz line noise or any of its harmonics (Fig. A.1; Step 9). The output of this analysis was a set of eight binary outcomes for each subject: 0 for each insignificant fiber response and 1 for each significant fiber response, defined as having an amplitude in a particular conduction band of the Letter System whose amplitude is significantly different from 0V at $\alpha = 0.05$. More specifically, these 8-digit codes represented the “nerve response signatures” from the left and right vagus nerve of each subject as a set of numbers that indicate a detectable response (1) or no detectable response (0) from left vagal Aβ, Aγ, Aδ, B fibers and right vagal Aβ, Aγ, Aδ, B fibers. Since the Aδ fiber conduction velocity range from our classification system (CV: 5-15 m/s) overlaps with the B fiber conduction velocity range (CV: 3-14 m/s), we limited the B fiber classification to only survey the signal from 3-5 m/s. The stimulus pulse frequency and long conduction distances (between 29 and 40 cm) prevented us from assessing the response data for any

form of C fiber activity as per the measurement protocol described above. If the circumstances of recording prevented us from resolving B fiber (or other) data, the corresponding position in the 8-digit code was left blank to avoid influencing the symptom parity analysis (Section 2.2.4). It is important to note that these conduction velocity estimates could be overestimating or underestimating the true values, because we could not directly measure the length of the nerve or the precise point of vagal activation. Care must therefore be taken to have one investigator consistently perform these measurements in the same manner. This approach ensures that the data can be treated equally within the confines of this protocol.

2.2.4. Method to detect associations among CNAP response and symptom score data—After the mean cutaneous vagal responses were processed and classified as described in Section 2.2.1–2.2.3 above, the GCSI symptom survey data, GES parameter settings, age, gender and disease etiology data were made available in order to identify whether features of the cutaneous vagal recordings predict differences in gastroparesis symptoms. All statistical analysis was performed with STATA 14.2 or R and verified with IRB biostatisticians. Using STATA 14.2, symptom scores were compared between groups of subjects with significant [$CNAP^{(+)}$] or without significant [$CNAP^{(-)}$] left or right vagal Aβ, Aγ, Aδ, or B fiber responses, defined as volleys in the mean response to GES whose peak amplitude is significantly different from 0 V at $\alpha = 0.05$. More specifically, we determined whether the difference in the mean symptom scores reported by patients with a particular type of nerve response and those without that same response was significantly different from 0 (at $\alpha < 0.05$). Potential outcomes of this analysis are described below:

- We expected no significant difference (or effect of vagal fibers) between the symptom scores reported by a subgroup of subjects with a detected vagal response and a subgroup of subjects without a detected vagal response if the signal detected from the cutaneous electrodes was
  - A) not involved in the mechanism of action of GES, or
  - B) not physiological (i.e., noise or other random fluctuations).
- In contrast, we expected a significantly lower mean symptom score in a subgroup of subjects with a particular type of fiber response if the signal detected from the cutaneous recording electrodes was
  - C) somehow involved in the mechanism of action of GES.
- Lastly, we expected a significantly higher mean symptom score (i.e., more frequent or severe) in a subgroup of subjects with a particular type of fiber response if the signal detected from the cutaneous recording electrodes was
  - D) somehow related to a side-effect of GES therapy.

The unpaired t-test with Welch approximation was used for all symptom parity comparisons, assuming unequal variances within the symptom data belonging to each subgroup. For all comparisons, data were reported as a difference in mean symptom scores among a subgroup with and without a particular fiber response to GES (mean ± s.e.m.). A negative number indicated that the subgroup with the particular fiber response shown on the x-axis labels

reported, on average, a less severe and/or frequent incidence of that symptom than those without the same fiber response profile.

3. Results

3.1. Noninvasive measurement of GES-evoked vagal CNAPs in human

Fig. 2A shows an example segment of an EKG (filtered to expose the GES stimulus artefacts), left vagal and right vagal recording used to detect the presence of evoked vagal nerve responses to GES therapy. The GES device is off from approximately 260 to 306 s into the recording, after which it is turned back on (indicated with a red bar).

Fig. 2B shows example cutaneous response data measured from a single patient while the stimulator was on and tuned to a stimulus pulse repetition frequency of 55 Hz, which made it easy to observe raw responses to a train of stimuli (top: stimulus artefacts detected from the high pass-filtered EKG trace; middle: cutaneous recording over the left vagus nerve; bottom: cutaneous recording over the right vagus nerve). Red arrows in Fig. 2B show the locations of the stimulus artefacts, which were detected offline from the filtered EKG trace with custom software and used to extract the segments of data following each stimulus. The cutaneous response to each stimulus was then averaged to boost the signal-to-noise ratio of the evoked response measured from the skin surface over the left and right cervical vagus nerve (Fig. 2C, which shows an example mean response from a different subject whose stimulus pulse frequency was set to 14 Hz).

Fig. 2D overlays the mean left vagal cutaneous response to gastric electrical stimulation as a function of conduction velocity for six subjects. The amplitude of each trace was normalized to the maximum amplitude within each trace to further highlight common features among responses from different subjects. The shaded regions denote the conduction velocity range associated with Aα (70-120 m/s), Aβ (40-70 m/s), Aγ (15-40 m/s), Aδ (5-15 m/s) and B (3-14 m/s) fibers in the Letter System (the C fiber conduction velocity range is not shown since its expected latency, on average, exceeds the latency between stimulus pulses delivered by the GES device). Note the prominence and consistency of the response peaks that fall within the Aβ/Aγ range (Fig. 2D; red dashed circle).

3.2. Study population characteristics

Of the 66 subjects included in this analysis, 28 had diabetic GP (type 1:9; type 2:19), 35 had idiopathic GP, and 3 had postsurgical GP. Subject demographics and stimulus parameter settings are summarized in Fig. 3 and Table A.1 of Appendix A. Mean stimulus parameter settings do not significantly differ according to gender or disease etiology (mean stimulus pulse current = 7.7 ± 3.46 mA). Further analysis and interpretation of these particular data is beyond the scope of this paper. GCSI symptom survey data are summarized in Table 1 by gender and disease etiology and graphically for the entire study population in Fig. 3.

3.3. Relationship between stimulus parameters, vagal CNAP features and symptom scores

We first performed a high-level regression analysis to determine whether A) stimulus pulse current/charge predicted changes in total symptom score (the sum of all severity and frequency scores for all 9 symptoms on the GCSI survey) (Fig. 4A–D; Left Column) and/or whether B) the degree of vagal recruitment (i.e., the sum of left and right vagal CNAP volleys in the mean left and right CNAP responses whose peaks are significantly different from 0 V at $\alpha = 0.05$) predicted changes in the total symptom score (Fig. 4E–H; Right Column). The degree of vagal recruitment was computed as the sum of the eight binary values assigned to the mean left and right vagal CNAP responses, respectively. If we detected no significant volleys in either the left or right vagal response, then the number of significant CNAP volleys was equal to 0. Similarly, if we detected only left vagal Aγ and B fiber volleys, along with right vagal B fiber volleys, then the number of significant CNAP volleys was equal to 3 (i.e., $LV_{A\beta}^{(-)} + LV_{A\gamma}^{(+)} + LV_{A\delta}^{(-)} + LV_{B}^{(+)} + RV_{A\beta}^{(-)} + RV_{A\delta}^{(-)} + RV_{A\delta}^{(-)} + RV_{B}^{(+)} = 0+1+0+1+0+0+0+1 = 3$).

Stimulus pulse current and charge per pulse did not predict total symptom scores [$F(1,56) = 0.11$; Prob > F = 0.737] (Fig. 4A), even when accounting for biological sex. There was a significant relationship between total number of significant left and right vagal CNAP volleys and total symptom score: As the total number of significant left and right vagal CNAP volleys increased, the observed total symptom score decreased [$F(1,49) = 4.68$; Prob > F = 0.035] (Fig. 4E). When accounting for biological sex, the trend remains, but not the statistical significance for males [$F(1,6) = 0.93$; Prob > F = 0.373] or females [$F(1,41) = 1.98$; Prob > F = 0.167].

Considering disease etiology, increasing stimulus charge per pulse predicted an increase (i.e., worsening) in total symptom score for type 1 diabetic subjects [$F(1,6) = 16.39$; Prob > F = 0.0067] (Fig. 4D), but did not predict any change for subjects with idiopathic [$F(1,28) = 0.02$; Prob > F = 0.90] (Fig. 4B) or type 2 diabetic gastroparesis [$F(1,15) = 0.22$; Prob > F = 0.648] (Fig. 4C). When accounting for biological sex and disease etiology, we no longer observed a significant predictive relationship between stimulus charge per pulse and total symptom score for male [$F(1,1) = 5.46$; Prob > F = 0.257] or female [$F(1,3) = 7.60$; Prob > F = 0.070] subjects with type 1 diabetes.

As the total number of significant vagal CNAP volleys increased, there was an associated and significant decrease in total symptom score in subjects with idiopathic gastroparesis [$F(1,25) = 6.04$; Prob > F = 0.021] (Fig. 4F). When accounting for biological sex and disease etiology, the same significant trend remained for male [$F(1,1) = 456.33$; Prob > F = 0.030] and female [$F(1,22) = 5.26$; Prob > F = 0.032] subjects with idiopathic gastroparesis; note, however, that there were only three males with idiopathic gastroparesis in this study. No relationship was observed when performing the same analysis on subjects with type 2 [$F(1,13) = 0.62$; Prob > F = 0.446] (Fig. 4G) or type 1 diabetic gastroparesis [$F(1,4) = 0.26$; Prob > F = 0.634] (Fig. 4H).

To determine more precisely whether specific fiber groups correlated with positive or negative changes in specific symptoms, we computed the difference in symptom severity

and frequency scores from subjects whose recordings showed the presence of a particular fiber group [$CNAP^{(+)}$] versus subjects whose recordings did not show the same response [$CNAP^{(-)}$] (Fig. 5). Fig. 5 shows the output of this analysis without considering disease etiology, where the net difference in scores are reported as GCSI scale points (i.e., a scale of 0-4). Note how the difference in symptom score was almost always negative using this analysis, which strongly suggested that the vagus was involved in mediating the therapeutic effects of GES therapy. Upon further inspection, it was clear that left vagal Aγ and B fibers, along with right vagal Aβ, Aδ and B fibers, played an important role in the mechanism of action of GES therapy, especially left vagal Aγ fibers.

A similar analysis was performed separately for nausea, vomiting and early satiety, according to disease etiology (Fig. 6). The output of the full analysis for each etiology is shown in Appendix A (Figs. A.2–A.4). In Fig. 6, we compared the output of the analysis of the effect of fiber activation on nausea, vomiting and early satiety symptom scores. Of note, the analysis showed that the type of vagal recruitment associated with symptom improvement differed according to etiology.

For subjects with idiopathic gastroparesis, left vagal Aγ fiber recruitment predicted a significant improvement in the severity and frequency of early satiety ($p < 0.05$, respectively). Right vagal Aβ fiber recruitment predicted a significant improvement in vomiting frequency ($p < 0.05$). Right vagal Aδ fiber recruitment predicted significant improvements in nausea frequency ($p < 0.05$), vomiting severity ($p < 0.01$) and vomiting frequency ($p < 0.01$). Right vagal B fiber recruitment predicted significant improvements in nausea severity and frequency ($p < 0.05$), vomiting severity and frequency ($p < 0.01$), and early satiety severity ($p < 0.05$).

For subjects with type 2 diabetic gastroparesis, fiber recruitment did not predict any significant improvement in nausea, vomiting or early satiety symptoms. In contrast: For type 1 diabetics, left vagal Aβ fiber recruitment predicted a significant increase (i.e., worsening) in the severity of early satiety symptoms ($p > 0.95$). This represented a potential side effect of GES therapy, consistent with the regression analysis that showed a significant increase in total symptom score as the energy delivered by the GES device increased. There was some potential benefit for type 1 diabetics, despite these apparent side effects: Left vagal Aγ fiber recruitment predicted a significant improvement in vomiting severity and frequency ($p < 0.05$). Left vagal B fiber recruitment predicted a significant improvement in nausea severity ($p < 0.01$) and early satiety frequency ($p < 0.05$). Right vagal Aδ and B fiber recruitment predicted a significant improvement in early satiety severity ($p < 0.01$) and frequency ($p < 0.05$).

3.4. Cohen's *d* analysis to estimate the net effects of therapeutic vagal recruitment with GES

Our previous analysis strongly pointed to vagal involvement in the mechanism of action of GES therapy in reducing the severity and frequency of specific symptoms common to gastroparesis. Cohen's *d* was next used as a standardized metric to estimate the size of the symptom-reducing effect attributed to particular types of vagal nerve responses (essentially, an unbiased measure of the difference in mean values of subjects with or without a particular

vagal response signature associated with their GES stimulus parameters). Any value greater than 0.8 is considered a large effect size. Any Cohen's *d* estimate whose 95% confidence interval does not include 0 is statistically significant [17, 18]. In Table 2, we show the output of the Cohen's *d* analysis performed in STATA 14 to compare differences in the severity and frequency of the 9 hallmark symptoms of gastroparesis with or without the candidate "optimal" vagal response signature. Similar tables for idiopathic, type 2 and 1 diabetic gastroparesis are shown in the Appendix A (Tables A.2–A.4, respectively). Using the analysis, we found that left vagal Aγ along with right vagal Aδ and B fibers were critical components of the treatment response to GES. When absent, subjects consistently reported higher (i.e., worse) symptom scores.

4. Discussion

4.1. Summary of findings

Through novel analytical methods, we have shown that it is possible to extract meaningful information from the vagus nerve in response to gastric electrical stimulation using simple, but well-placed cutaneous electrodes, and a methodical, progressive method of data reduction for comparative analyses (Fig. 7). We have shown that stimulus parameters do not predict any change in symptom scores outside of predicting a substantial increase (i.e., worsening) in the total symptom score for type 1 diabetics as the charge per stimulus pulse increases ($p = 0.0067$) (we can treat the charge per pulse as interchangeable with the stimulus pulse current, because the stimulus pulse duration is almost always fixed at 330 μs). In contrast, we showed that there is a significant reduction in total symptom scores as the total number of classes of fibers (left plus right) that show significant signals when the gastric electrodes were activated increased ($p = 0.035$). This same relationship held for subjects with idiopathic gastroparesis ($p = 0.021$), but not for subjects with diabetic gastroparesis. Taken together, we conclude that the vagus is an essential component of the mechanism of action of GES therapy, especially for subjects with idiopathic or type 1 diabetic gastroparesis. The presence of side effects attributed to the activation of certain fiber groups in type 1 and 2 diabetic subjects underscores the utility of our approach and the need to develop feedback systems that can enable fine-tuning of the nerve response that predicts a positive therapeutic response to GES therapy in each subject (even though the stimulus parameters required to recruit the desired nerve response will likely differ across subjects and perhaps within the same subjects over time).

4.2. Potential sources of signals measured overlying the mid-cervical vagal nerves

The GES electrodes are implanted 10 cm proximal to the pylorus along the greater curvature of the stomach. The bipolar stimulating electrodes are implanted approximately 1 cm apart with a slight bias toward the anterior (or ventral) wall of the stomach. Fig. 8 shows the approximate location of these implanted GES electrodes in relation to the anterior nerve of Laterjet, which arises from the anterior gastric branch of the anterior abdominal vagal trunk, and in relation to the pyloric branch(es) of the vagus nerve, which arise from the hepatic branch of the anterior abdominal vagal trunk to supply the pylorus.

Based on the location of the stimulating electrodes, the signals that we measure from the skin surface overlying the left cervical vagus nerve would most likely come from fibers contained within the branches that project from the anterior nerve of Laterjet near the junction of the corpus and pyloric antrum. The source of the signals observed overlying the right cervical vagus nerve is less certain, since the electrodes are implanted on the ventral wall of the stomach, which we expect would only produce action potentials that could be observed along the left vagus nerve. While deriving the true source of these right vagal signals is beyond the scope of this work, we can speculate that the right vagal signal is due to 1) direct activation of dorsal gastric fibers resulting from the large stimulus currents employed in GES (unlikely), 2) crosstalk between the left and right vagus nerve via communicating branches that are believed (but to our knowledge not proven in human subjects) to exist within the esophageal plexus [19], 3) as a result of vagal reflexes initiated by left vagal afferent activation (which could perhaps result in an efferent signal from the right vagus nerve), or 4) some other unknown source.

4.3. Forward-looking statements

A collaborative effort involving experts from highly disparate, specialized disciplines is needed to develop diagnostic and therapeutic technology that is safe, effective, easy to use, and well-tailored to control symptomatic gastroparesis. The Medtronic Enterra Neurostimulator is the only GES device available to patients with treatment-resistant diabetic or idiopathic gastroparesis. It is approved under a Humanitarian Device Exemption. While safe and moderately effective in select patients, there is no objective method to optimize the parameters of stimulation in a timely, efficient manner, especially in a manner that produces predictable changes in symptom profiles. The conventional approach is to fit the patient to the device. Our end goal is to develop an intelligent device that conforms itself to the patient, simultaneously simplifying the selection of optimal stimulus parameters and improving the efficacy of the therapy. In this approach, a computer is programmed to monitor the efficacy of therapy and to adjust stimulus parameters, within safe limits, such that the efficacy of therapy is maintained over time.

Effective, translatable technologies are designed for the patient and physician. Gastroenterologists understand the gaps in treatment, while engineers understand the gaps in technology. **In stark contrast to the conventional *one-size-fits-all* approach to biomedical device design, we have taken steps toward the development of a *one-size-fits-one* approach**. If afferent vagal nerve conduction mediates the therapeutic effect of GES, then directly recruiting the same patterns of vagal nerve activity via vagal nerve stimulation represents a more efficient and direct method of treatment for idiopathic and diabetic gastroparesis. Here, we show strong preliminary data that suggest the vagal CNAP response, presumed to be a measure of afferent vagal nerve activation in response to GES, is a promising response marker of GES treatment efficacy, and that the CNAP response can be detected through the skin surface.

4.4. Limitations of approach

Potential limitations of our approach are:

1. Vagal afferents are the presumed mediators of effective and ineffective GES therapy. The potential influence of sympathetic nerves or hormones are not considered.
2. The compound nerve action potential from afferent vagal nerve activation may not be measurable from the skin surface in all patients due to differing anatomical paths of the cervical vagus, different amounts of adiposity, or severe neuropathy. When it is measurable, a low signal-to-noise ratio may preclude its utility as a robust marker of GES efficacy. Fig. A.5 of Appendix A shows a basic regression analysis of the area-under-the-curve of rectified left and right vagal responses (in μV s) with respect to BMI (in kg/m^2). While the observed trends were not statistically significant for any of the fiber groups, the analysis suggested that the ability to detect GES-evoked signals measured overlying the left and right cervical vagal nerves would be lost when recording from subjects whose BMI is greater than approximately 35-40 kg/m^2.
3. Additional tests may be needed to identify vagal nerve damage or neuropathy due to complications from diabetes. These tests may be invasive.
4. It is not possible to precisely measure conduction distance in a noninvasive manner. However, this limitation can be overcome through the use of multichannel electrode systems with precise interelectrode distances.

5. Conclusions

Vagal CNAP analysis is a useful technique to define relationships among GES parameters, vagal recruitment, efficacy and side-effect management. Our results suggest that CNAP-guided GES optimization will provide the most benefit to patients with idiopathic and type 1 diabetic gastroparesis, especially when tuned for left vagal Aγ and right vagal Aδ/B fiber responses, which consistently predict symptom score improvements. The side effects associated with left vagal Aβ activation in type 1 diabetics underscore the need to consider disease etiology in the patient and parameter selection process.

Supplementary Material

Refer to Web version on PubMed Central for supplementary material.

Acknowledgments

This study was funded by the NIH Stimulating Peripheral Activity to Relieve Conditions (SPARC) program (OT2OD023847). We would like to thank Dr. Pedro Irazoqui for his role in shaping the early phase of this project and Dr. Mary Ann Montero for her assistance in identifying validated visual analog scales to capture symptom profile data. We would also like to thank Ms. Keaton Poppe for her assistance with data analysis and Mr. Jongcheon Lim for his custom illustrations in Fig 1.

References

[1]. Camilleri M, “Clinical Practice: Diabetic Gastroparesis,” N Engl J Med, vol. 356, no. 8, pp. 820–829, 2007. [PubMed: 17314341]

[2]. Soykan I, B. S, Sarosiek I et al., “Demography, clinical characteristics, psychological and abuse profiles, treatment, and long-term follow-up of patients with gastroparesis,” Digestive Diseases and Sciences, vol. 43, no. 11, pp. 2398–2404, 1998. [PubMed: 9824125]

[3]. Camilleri M, Bharucha AE, and Farrugia G, “Epidemiology, mechanisms, and management of diabetic gastroparesis,” Clinical Gastroenterology and Hepatology, vol. 9, no. 1, pp. 5–12, 2011. [PubMed: 20951838]

[4]. Ward MP, Nowak TV, Irazoqui PP et al., “Gastric Electrical Stimulation of the Antrum Evokes Compound Cervical Vagal Nerve Action Potentials in Rodents,” Gastroenterology, vol. 148, no. 4, pp. S507, 2015.

[5]. Bilgutay AM, Wingrove R, Griffin WO et al., “Gastro-intestinal pacing: A new concept in the treatment of ileus,” Annals of Surgery, vol. 158, no. 3, pp. 338–347, 1963. [PubMed: 14061702]

[6]. Bellahsene BE, Lind CD, Schirmer BD et al., “Acceleration of gastric emptying with electrical stimulation in a canine model of gastroparesis,” Am J Physiol, vol. 262, pp. G826–G834, 1992. [PubMed: 1590392]

[7]. Eagon JC, and Kelly KA, “Effects of gastric pacing on canine gastric motility and emptying,” Am J Physiol, vol. 265, pp. G767–G774, 1993. [PubMed: 8238360]

[8]. Lin ZY, McCallum RW, Schirmer BD et al., “Effects of pacing parameters on entrainment of gastric slow waves in patients with gastroparesis,” Am J Physiol, vol. 274, pp. G186–G191, 1998. [PubMed: 9458788]

[9]. McCallum RW, Chen JDZ, Lin Z et al., “Gastric pacing improves emptying and symptoms in patients with gastroparesis,” Gastroenterology, vol. 114, pp. 456–461, 1998. [PubMed: 9496935]

[10]. Familoni BO, Abell TL, Nemoto D et al., “Efficacy of electrical stimulation at frequencies higher than basal rate in canine stomach,” Digestive Diseases and Sciences, vol. 42, no. 5, pp. 892–897, 1997. [PubMed: 9149039]

[11]. Familoni BO, Abell TL, Voeller G et al., “Case Report: Electrical stimulation at a frequency higher than basal rate in human stomach,” Digestive Diseases and Sciences, vol. 42, no. 5, pp. 885–891, 1997. [PubMed: 9149038]

[12]. Xing J, Brody F, Rosen M et al., “The effect of gastric electrical stimulation on canine gastric slow waves,” Am J Physiol Gastrointest Liver Physiol, vol. 284, pp. G956–G962, 2003. [PubMed: 12584109]

[13]. Payne SC, Furness JB, and Stebbing MJ, “Bioelectric neuromodulation for gastrointestinal disorders: effectiveness and mechanisms,” Nat Rev Gastroenterol Hepatol, vol. 16, no. 2, pp. 89–105, 2019. [PubMed: 30390018]

[14]. Revicki DA, Rentz AM, Dubois D et al., “Development and validation of a patient-assessed gastroparesis symptom severity measure: The Gastroparesis Cardinal Symptom Index,” Aliment Pharmacol Ther, vol. 18, pp. 141–150, 2003. [PubMed: 12848636]

[15]. Abell TL, Van Cutsem E, Abrahamsson H et al., “Gastric Electrical Stimulation in Intractable Symptomatic Gastroparesis,” Digestion, vol. 66, pp. 204–212, 2002. [PubMed: 12592096]

[16]. Gasser HS, “The Classification of Nerve Fibers,” Ohio J Sci, vol. 41, pp. 145–159, 1941.

[17]. Cohen J, “The statistical power of abnormal psychological research: a review,” Journal of Abnormal Social Psychology, vol. 65, pp. 145–153, 1962. [PubMed: 13880271]

[18]. Cohen J, Statistical power analysis for the behavioral sciences, 2nd ed., Hillsdale, NJ: Lawrence Erlbaum Associates, 1988.

[19]. Horn CC, Meyers K, Lim A et al., “Delineation of vagal emetic pathways: Intragastric copper sulfate-induced emesis and viral tract tracing in musk shrews,” Am J Physiol Regul Integr Comp Physiol, vol. 306, pp. R341–R351, 2014. [PubMed: 24430885]

Highlights

- Increased vagal activity with GES predicts lower total symptom scores ($p < 0.05$)
- These vagal responses to GES can be detected with cutaneous electrodes
- GES parameters do not predict gastroparesis symptom relief, but vagal responses do
- Left vagal Aγ and right vagal Aδ/B fiber activation predict effective GES therapy
- Disease etiology is an important predictor of treatment response to GES therapy

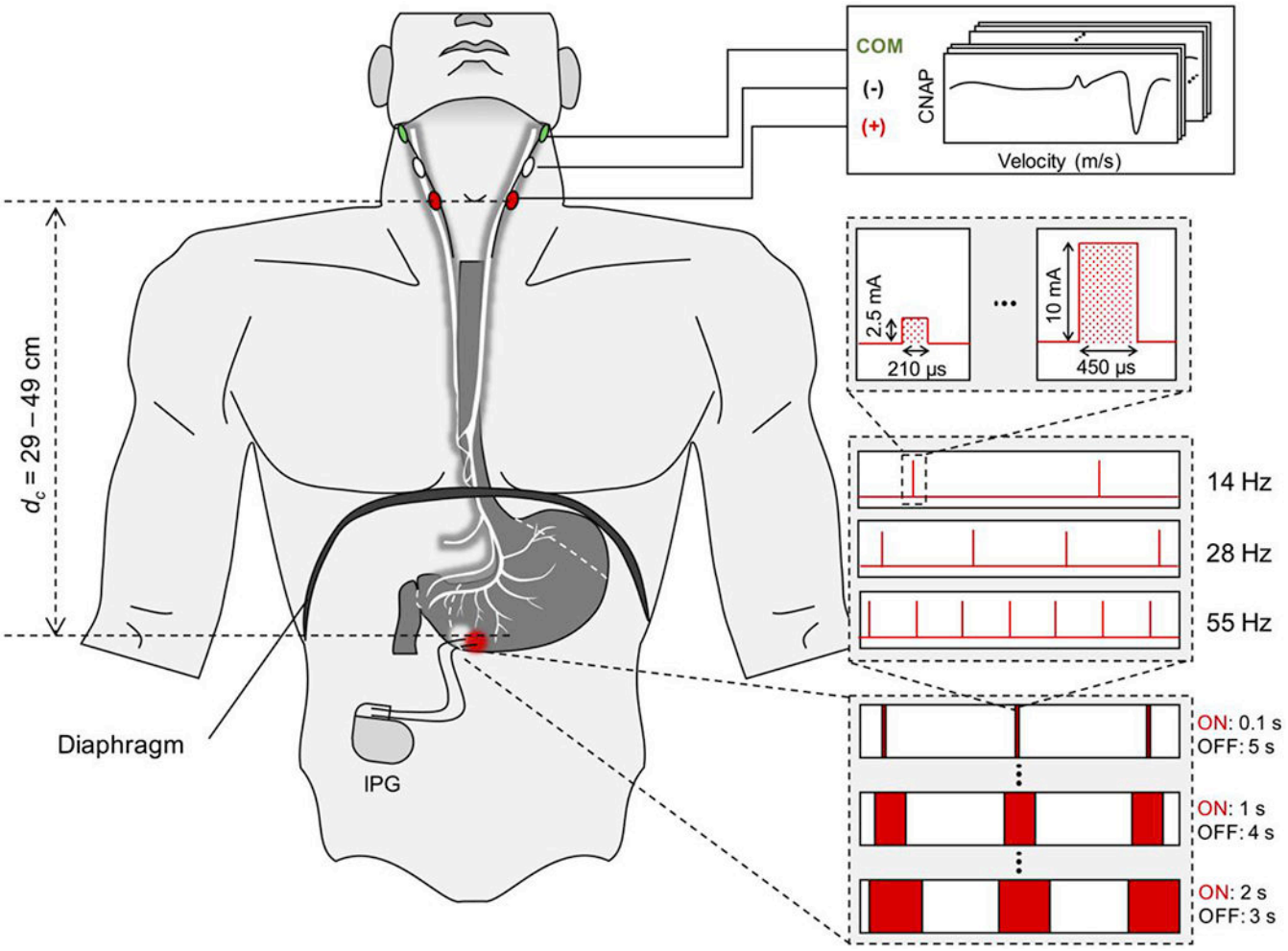

Fig. 1.

Gastric electrical stimulation and cutaneous vagal recording electrode placement. Graphical overview of GES electrode implant location, cutaneous recording electrode placement and available stimulus parameter settings [Image generated by Jongcheon Lim, Purdue University, 2020].

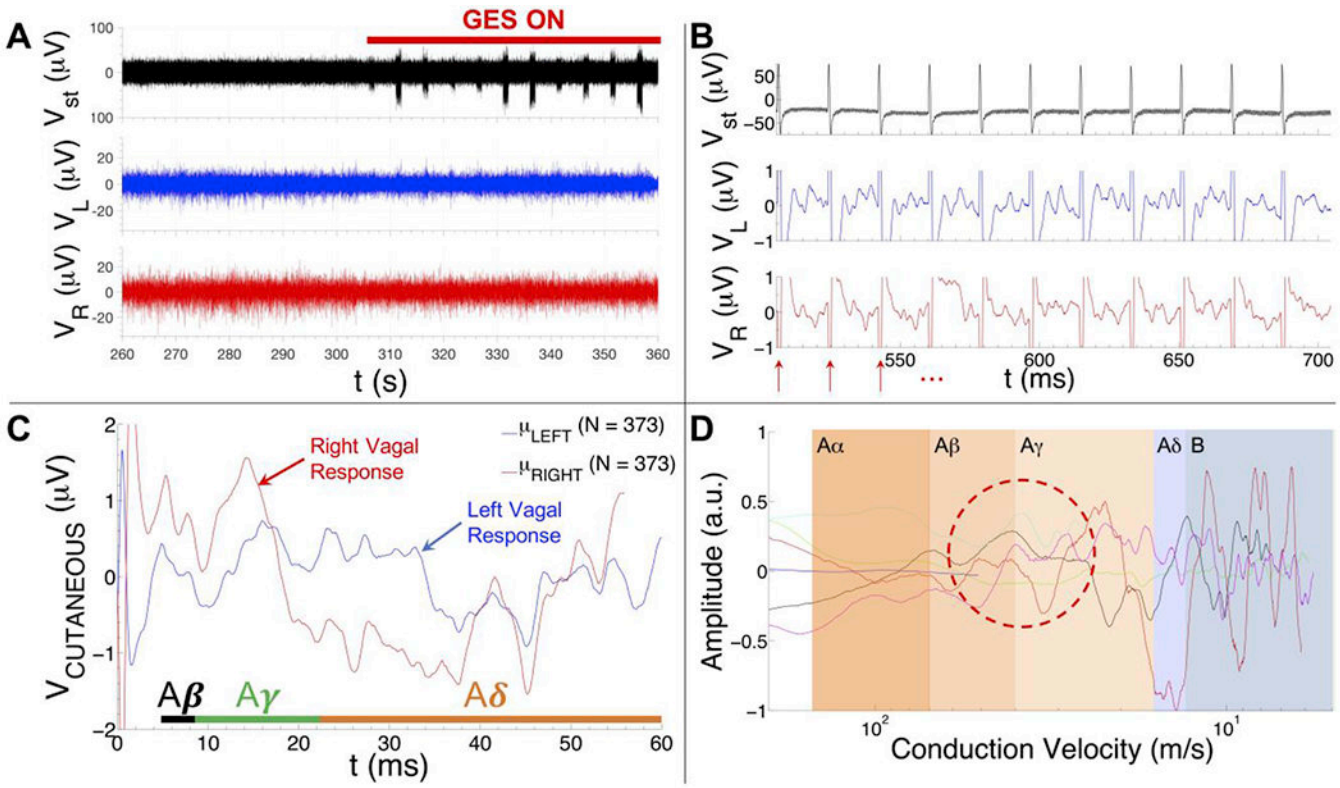

Fig 2.

Summary of GES-associated signal processing pipeline. **A**) Cutaneous recordings were collected with an 8-channel PowerLab system (AD Instruments) using the cutaneous recording electrode placements from Fig. 1. A 100 s long segment of a high pass-filtered EKG (top trace), left vagal (middle trace) and right vagal (bottom trace) recording is shown from one subject (v003). The GES device is turned on at ~306 s in the recording (red bar). **B**) Representative data collected from one subject (subject v003) whose GES device was on and tuned to a pulse repetition frequency of 55 Hz (top: stimulus artefacts detected from the high pass-filtered EKG trace; middle: cutaneous recording over the left vagus nerve; bottom: cutaneous recording over the right vagus nerve). Red arrows show the stimulus artefact locations. Raw response data associated with GES is visible in the left vagal (middle row) and right vagal (bottom row) channels during the 18 ms intervals between stimulus artefacts. **C**) Mean cutaneous response recorded over the left (blue trace) and right vagus (red trace) nerve of another subject (subject v011) whose GES device was on and tuned to a pulse repetition frequency of 14 Hz (mean of N = 373 responses). The time intervals where one would expect to find Aβ, Aγ and Aδ fiber responses are shown in the plot (time intervals were computed using the 33 cm conduction distance for subject v011). **D**) Mean left vagal cutaneous response to gastric electrical stimulation as a function of conduction velocity (i.e., speed) for six human subjects (normalized to the maximum response voltage detected among all six traces to aid visual comparison). Note that the blue trace only extends into the Aβ range and the light blue/cyan trace only extends into the Aγ range. These traces are from subjects whose prescribed stimulus pulse repetition frequency was tuned to 55 Hz (blue) and 28 Hz (light blue/cyan), respectively, as opposed to the typical value of 14 Hz. The red

dashed oval is intended to highlight the relative consistency of the left vagal Aγ volley observed in different subjects.

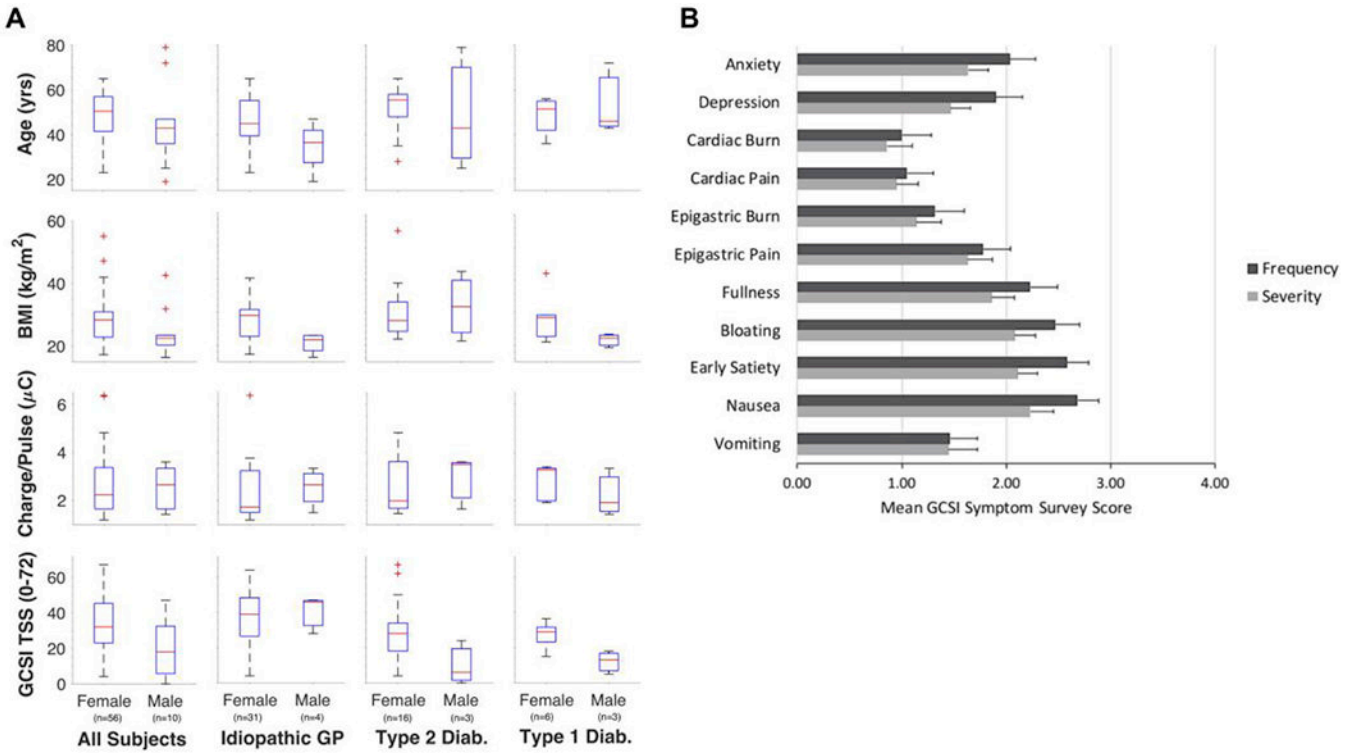

Fig. 3.

Summary of subject age, body mass index, stimulus strength and Gastroparesis Cardinal Symptom Index (GCSI) Survey results by biological sex and etiology. **A)** Summary of subject age, BMI (in kg/m^2), stimulus strength (in μC per pulse), and total symptom score (TSS) for all subjects (column 1), subjects with idiopathic gastroparesis (column 2), subjects with type 2 diabetic gastroparesis (column 3), and subjects with type 1 diabetic gastroparesis (column 4). **B**) Graphical summary of symptom survey results from all 66 subjects included in this analysis. A one-item anxiety and depression survey was given to 40 of 66 subjects to determine whether mental health factors should be considered when interpreting associations between detected nerve responses and symptom profiles.

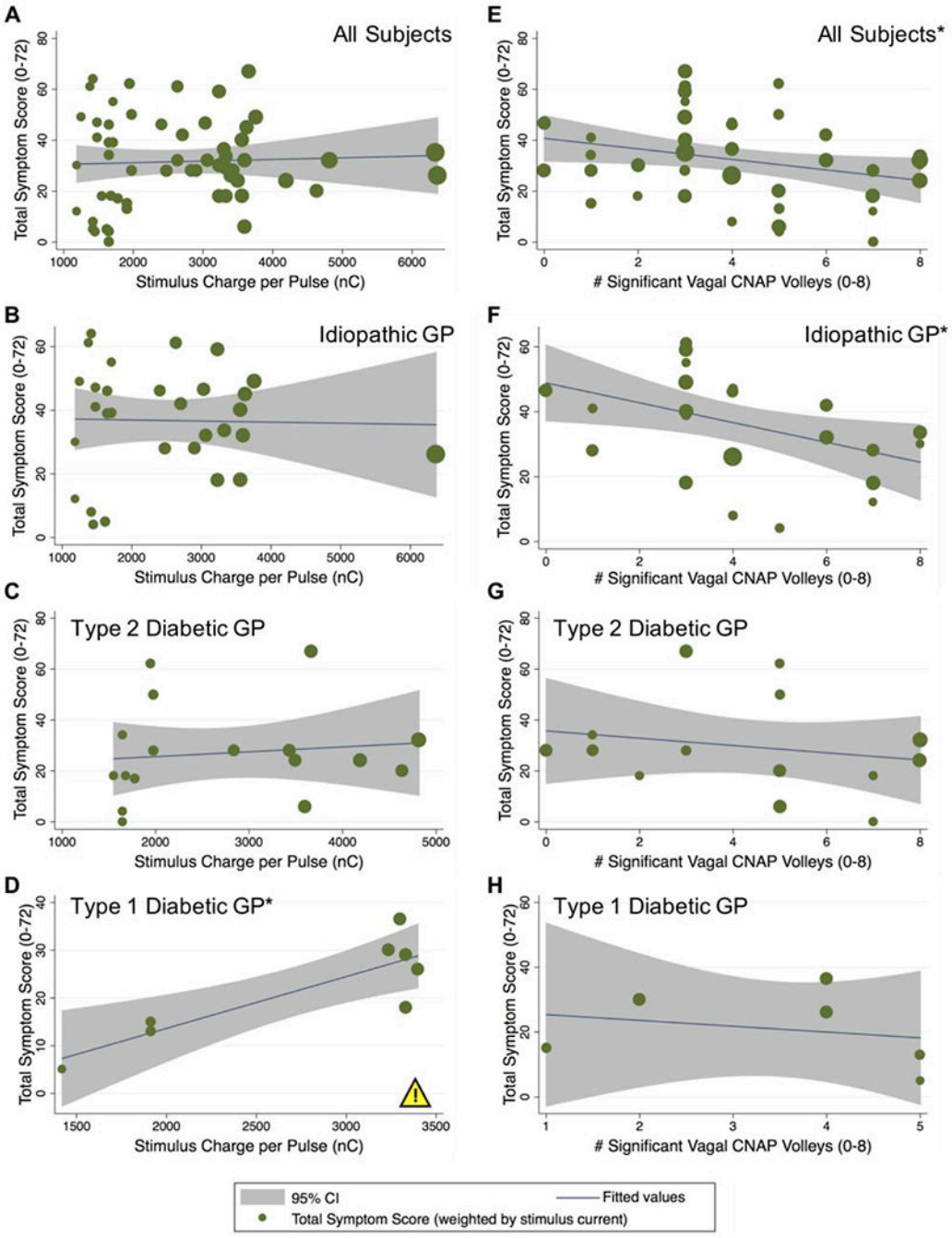

Fig. 4.

Effect of stimulus strength and fiber recruitment on total GCSI symptom score. Regression analysis to determine if stimulus charge per pulse and/or fiber recruitment number predict improvements in total GCSI symptom scores. **A-D**: Total symptom score versus stimulus charge per pulse (in nC) for all (N = 66) subjects (A), the n = 35 subjects with idiopathic gastroparesis (B), the n = 19 subjects with type 2 diabetic gastroparesis (C), or the n = 9 subjects with type 1 diabetic gastroparesis (D). Increasing stimulus charge per pulse predicted a higher total symptom score in type 1 diabetics ($p < 0.01$), suggesting a

worsening of their condition rather than an improvement as more energy is delivered. **E-H**: Total symptom score versus the total number of significant CNAP volleys from the left and right vagal recordings (0-8) for all N = 66 subjects (E), for n = 35 subjects with idiopathic gastroparesis (F), for n = 19 subjects with type 2 diabetic gastroparesis (G), or for n = 9 subjects with type 1 diabetic gastroparesis (H). Increasing the number of significant CNAP volleys predicted a significant decrease in total symptom score for all subjects (E) (*$p <$ 0.05) and for subjects with idiopathic gastroparesis (F) (*$p < 0.05$), suggesting an improvement in their condition with greater recruitment of the vagus. The yellow warning/caution icon highlights a potential side effect of stimulation observed among type 1 diabetic subjects, inferred from a statistically significant increase in symptom score with increasing stimulus intensity.

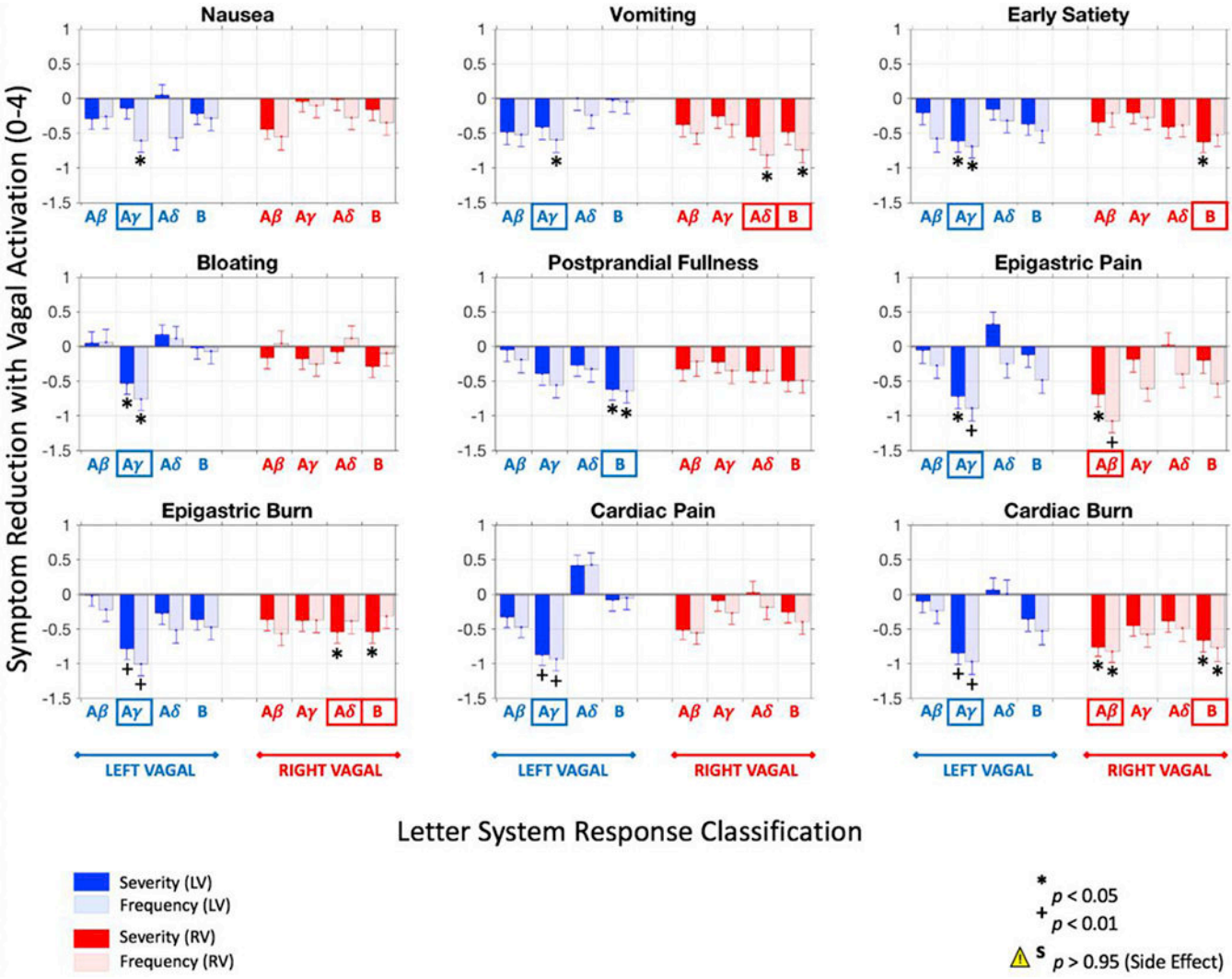

Fig. 5.

Gastroparesis symptom score improvement to (all subjects). GP symptom score improvement in subjects whose gastric electrical stimulation (GES) parameters are associated with left and/or right vagal fiber activation compared to those without the same type of vagal response (N = 66 subjects). Specifically, left vagal Aγ and B fibers, along with right vagal Aβ, Aδ and B fibers, were strongly associated with subjects reporting lower symptom scores on their GCSI survey, warranting further investigation into the role of these vagal responses in the mechanisms of GES therapy. Considering all of the symptom types and fiber groups, GES-evoked vagal activity was almost universally associated with subjects reporting lower symptom score ratings. Data are reported as *mean difference in symptom scores ± s.e.m.*

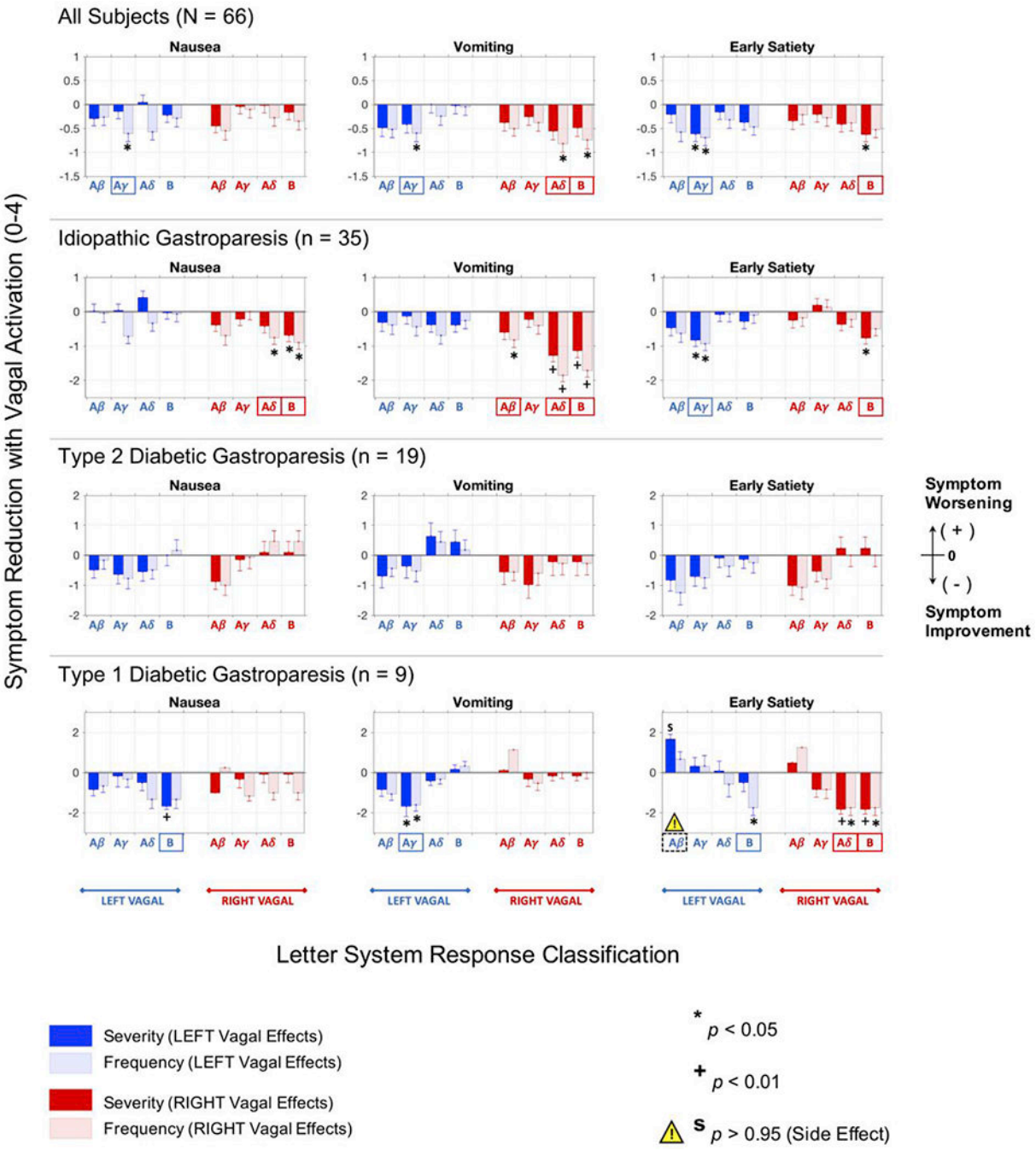

Fig. 6.

Symptom improvement with GES differs by disease etiology. Effect of disease etiology on GP symptom score improvement in subjects whose GES parameters are associated with left and right vagal activation compared to those without the same type of vagal response. The top row shows symptom score improvements associated with particular types of vagal response features for all subjects (N = 66 subjects) without considering disease etiology. Rows 2-4 show symptom score improvements for subjects with idiopathic GP (n = 35 subjects), subjects with type 2 diabetic GP (n = 19 subjects), and subjects with type 1

diabetic GP (n = 9 subjects), respectively. In almost every instance, GES-evoked vagal activity was associated with subjects reporting lower symptom score ratings. Note the difference in scale on the y-axes, which highlights the dramatic difference in response to GES among subjects with idiopathic, type 2 diabetic, or type 1 diabetic GP. For type 1 diabetic GP, left vagal Aβ fiber recruitment with GES predicted a significant worsening in the severity of their early satiety symptoms. Data are reported as *mean difference in symptom scores ± s.e.m.*

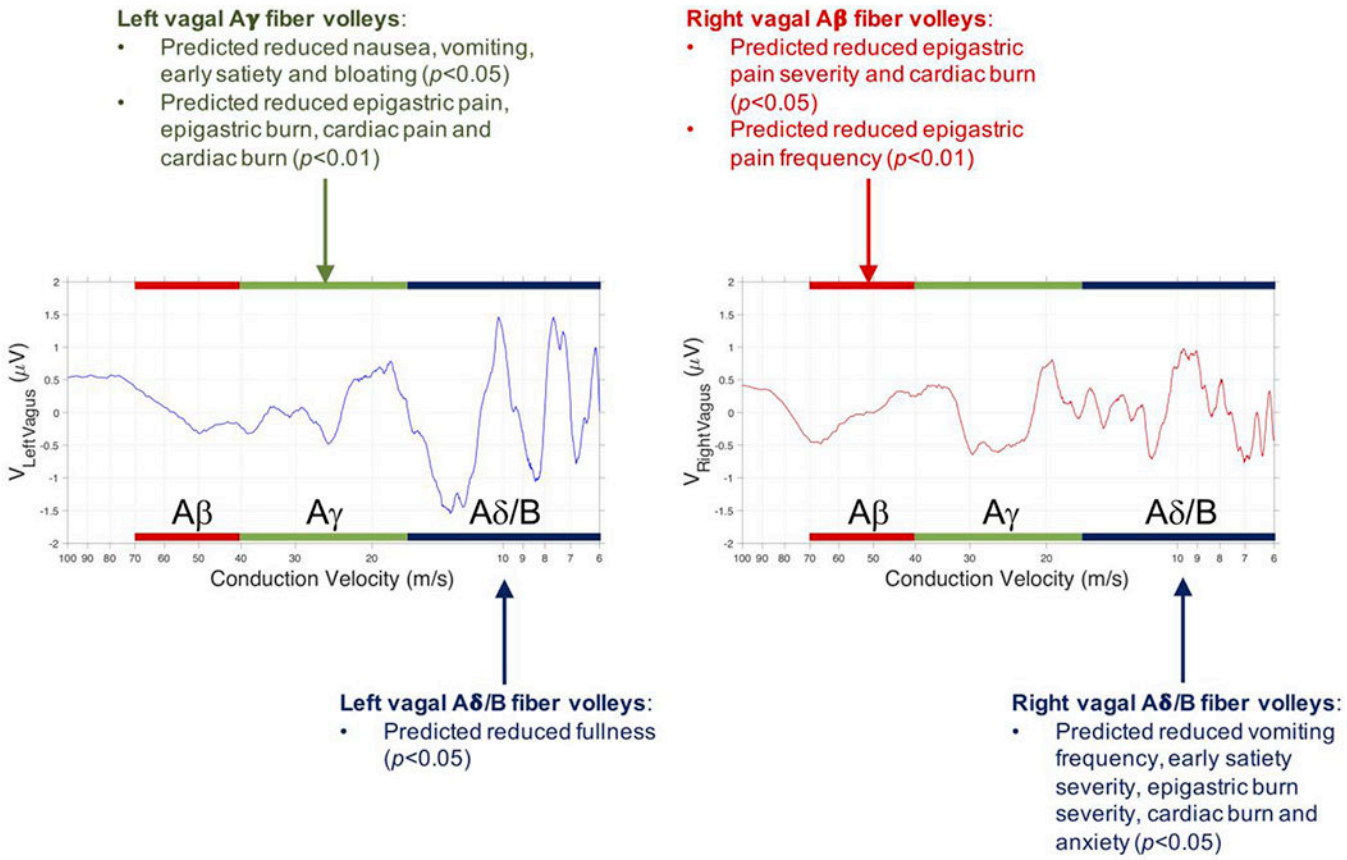

Fig. 7.

High level summary of the predicted nerve fiber population characteristics whose activity correlates with improvements in specific symptoms of gastroparesis. Summary data is plotted over data from one subject whose data showed significant fiber recruitment in all left and right vagal fiber groups considered in the analysis. The *p*-values refer to analyses performed with all N = 66 subjects included in the study.

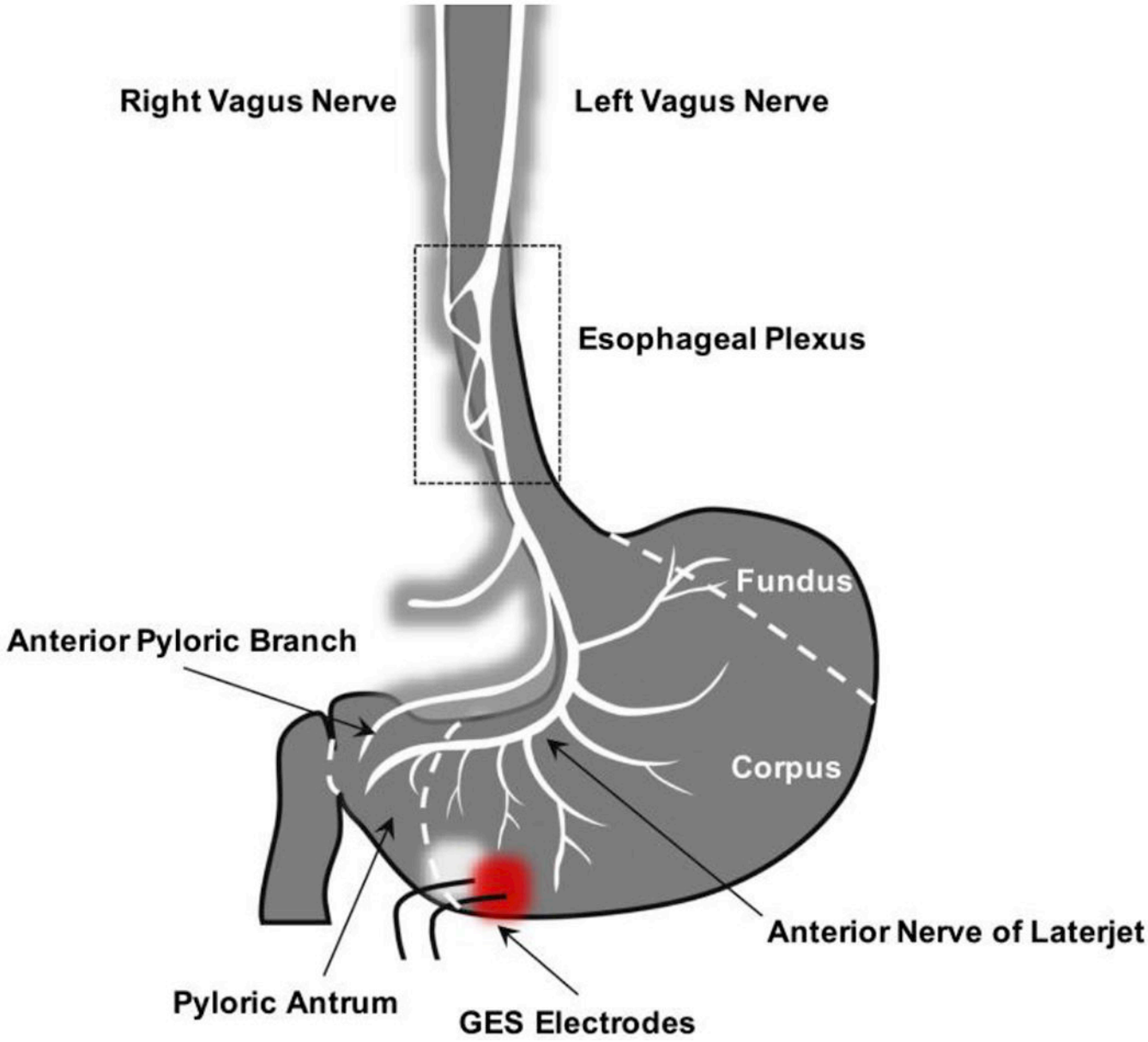

Fig. 8.
GES electrode location in relation to the nerves of the anterior abdominal wall.

Table 1

Gastroparesis Cardinal Symptom Index (GCSI) survey response summary[a]

GCSI Symptom Descriptors		Sex	Type 1 Diab.	Type 2 Diab.	Idiopathic	Postsurgical	Combined
Nausea	*Frequency*	M	1.67 ± 1.15	1.33 ± 1.15	3.25 ± 0.96	-	2.20 ± 1.32
		F	1.83 ± 1.17	2.67 ± 1.40	3.00 ± 1.31	3.00 ± 1.00	2.77 ± 1.32
		M + F	1.78 ± 1.09	2.44 ± 1.42	3.03 ± 1.26	3.00 ± 1.00	**2.68 ± 1.33**
	Seventy	M	2.67 ± 1.53	1.33 ± 1.15	2.75 ± 0.50	-	2.30 ± 1.16
		F	1.50 ± 0.84	2.13 ± 1.36	2.47 ± 1.09	1.67 ± 1.15	2.22 ± 1.17
		M + F	1.89 ± 1.17	2.00 ± 1.33	2.50 ± 1.04	1.67 ± 1.15	**2.23 ± 1.16**
Vomiting	*Frequency*	M	1.33 ± 1.53	0.33 ± 0.58	2.25 ± 0.96	-	1.40 ± 1.26
		F	0.80 ± 0.84	1.29 ± 1.33	1.72 ± 1.35	1.00 ± 1.00	1.47 ± 1.30
		M + F	1.00 ± 1.07	1.12 ± 1.27	1.78 ± 1.31	1.00 ± 1.00	**1.46 ± 1.28**
	Severity	M	1.67 ± 2.08	1.33 ± 2.31	2.00 ± 1.15	-	1.70 ± 1.64
		F	0.50 ± 0.55	1.50 ± 1.55	1.56 ± 1.19	1.00 ± 1.00	1.40 ± 1.27
		M + F	0.89 ± 1.27	1.47 ± 1.61	1.61 ± 1.18	1.00 ± 1.00	**1.45 ± 1.32**
Early Satiety	*Frequency*	M	0.67 ± 1.15	0.00 ± 0.00	3.00 ± 1.15	-	1.40 ± 1.65
		F	2.50 ± 1.05	2.80 ± 1.15	2.87 ± 1.28	2.67 ± 1.53	2.80 ± 1.21
		M + F	1.89 ± 1.36	2.33 ± 1.50	2.89 ± 1.25	2.67 ± 1.53	**2.58 ± 1.37**
	Severity	M	0.33 ± 0.58	0.00 ± 0.00	2.75 ± 0.50	-	1.20 ± 1.40
		F	2.17 ± 0.75	2.06 ± 1.24	2.39 ± 1.20	2.33 ± 1.15	2.27 ± 1.15
		M + F	1.56 ± 1.13	1.74 ± 1.37	2.43 ± 1.14	2.33 ± 1.15	**2.11 ± 1.24**
Bloating	*Frequency*	M	0.67 ± 1.15	0.67 ± 1.15	2.50 ± 1.29	-	1.40 ± 1.43
		F	2.25 ± 1.54	2.73 ± 1.10	2.65 ± 1.35	3.33 ± 0.58	2.67 ± 1.26
		M + F	1.72 ± 1.56	2.39 ± 1.33	2.63 ± 1.32	3.33 ± 0.58	**2.47 ± 1.36**
	Severity	M	0.67 ± 1.15	0.67 ± 1.15	1.50 ± 0.58	-	1.00 ± 0.94
		F	2.00 ± 1.41	2.25 ± 1.18	2.26 ± 1.18	3.00 ± 0.00	2.27 ± 1.17
		M + F	1.56 ± 1.42	2.00 ± 1.29	2.17 ± 1.15	3.00 ± 0.00	**2.08 ± 1.22**
Fullness	*Frequency*	M	0.67 ± 1.15	0.33 ± 0.58	3.00 ± 1.00	-	1.33 ± 1.50
		F	2.17 ± 1.33	2.53 ± 1.36	2.45 ± 1.43	1.33 ± 1.15	2.38 ± 1.38
		M + F	1.67 ± 1.41	2.17 ± 1.50	2.50 ± 1.40	1.33 ± 1.15	**2.23 ± 1.43**
	Severity	M	1.00 ± 1.00	0.33 ± 0.58	2.33 ± 0.58	-	1.22 ± 1.09
		F	1.83 ± 1.17	1.81 ± 1.17	2.16 ± 1.32	1.00 ± 1.00	1.96 ± 1.25
		M + F	1.56 ± 1.13	1.58 ± 1.22	2.18 ± 1.27	1.00 ± 1.00	**1.86 ± 1.25**
Epigastric Pain	*Frequency*	M	0.33 ± 0.58	0.67 ± 1.15	1.75 ± 2.06	-	1.00 ± 1.49
		F	1.33 ± 1.63	1.53 ± 1.51	2.18 ± 1.38	2.33 ± 1.53	1.92 ± 1.45
		M + F	1.00 ± 1.41	1.39 ± 1.46	2.13 ± 1.44	2.33 ± 1.53	**1.78 ± 1.48**
	Severity	M	0.33 ± 0.58	1.33 ± 2.31	1.50 ± 1.73	-	1.10 ± 1.60
		F	1.00 ± 1.26	1.50 ± 1.51	2.00 ± 1.36	1.67 ± 0.58	1.73 ± 1.38
		M + F	0.78 ± 1.09	1.47 ± 1.58	1.94 ± 1.39	1.67 ± 0.58	**1.63 ± 1.42**
Epigastric Burn	*Frequency*	M	0.00 ± 0.00	0.00 ± 0.00	1.25 ± 1.50	-	0.50 ± 1.08
		F	1.67 ± 1.63	1.27 ± 1.33	1.50 ± 1.42	1.67 ± 1.53	1.46 ± 1.39
		M + F	1.11 ± 1.54	1.06 ± 1.30	1.47 ± 1.41	1.67 ± 1.53	**1.32 ± 1.39**

GCSI Symptom Descriptors		Sex	Type 1 Diab.	Type 2 Diab.	Idiopathic	Postsurgical	Combined
	Severity	M	0.00 ± 0.00	0.00 ± 0.00	1.25 ± 1.50	-	0.50 ± 1.08
		F	1.67 ± 1.37	1.06 ± 1.24	1.23 ± 1.20	1.67 ± 1.53	1.25 ± 1.22
		M + F	1.11 ± 1.36	0.89 ± 1.20	1.23 ± 1.21	1.67 ± 1.53	**1.14 ± 1.23**
Cardiac Pain	*Frequency*	M	0.00 ± 0.00	0.33 ± 0.58	1.50 ± 1.73	-	0.70 ± 1.25
		F	1.00 ± 0.63	1.20 ± 1.52	1.10 ± 1.42	1.00 ± 1.00	1.11 ± 1.34
		M + F	0.67 ± 0.71	1.06 ± 1.43	1.14 ± 1.44	1.00 ± 1.00	**1.05 ± 1.33**
	Severity	M	0.00 ± 0.00	0.67 ± 1.15	1.25 ± 1.26	-	0.70 ± 1.06
		F	1.00 ± 0.63	1.13 ± 1.45	0.97 ± 1.30	0.67 ± 0.58	1.00 ± 1.25
		M + F	0.67 ± 0.71	1.05 ± 1.39	1.00 ± 1.28	0.67 ± 0.58	**0.95 ± 1.22**
Cardiac Burn	*Frequency*	M	0.00 ± 0.00	0.33 ± 0.58	1.25 ± 1.50	-	0.60 ± 1.07
		F	1.00 ± 1.26	1.13 ± 1.60	1.03 ± 1.56	1.33 ± 1.53	1.07 ± 1.50
		M + F	0.67 ± 1.12	1.00 ± 1.50	1.06 ± 1.54	1.33 ± 1.53	**1.00 ± 1.45**
	Severity	M	0.00 ± 0.00	0.33 ± 0.58	1.25 ± 1.50	-	0.60 ± 1.07
		F	1.00 ± 1.26	1.00 ± 1.32	0.84 ± 1.39	1.00 ± 1.00	0.91 ± 1.31
		M + F	0.67 ± 1.12	0.89 ± 1.24	0.89 ± 1.39	1.00 ± 1.00	**0.86 ± 1.28**

[a]Data reported as *mean ±st. dev.* (see row 1 of Table A.1 for sample size data)

Table 2

Effect of GES-evoked vagal signatures on symptom improvement (Cohen's *d* analysis)[a]

GCSI Symptom	Vagal Responses Linked to GES Efficacy								Effect Size (Cohen's *d*) Symptom *Severity*	Effect Size (Cohen's *d*) Symptom *Frequency*
	LEFT VAGUS				RIGHT VAGUS					
	Aβ	Aγ	Aδ	B	Aβ	Aγ	Aδ	B		
Nausea		◦							0.12 [−0.38, 0.62]	0.46 [−0.06, 0.97]
Vomiting		◦					•	•	**0.86 [0.04, 1.65]**	**1.18 [0.28, 2.06]**
Early Satiety		◦						•	**0.97 [0.16, 1.76]**	**0.83 [0.05, 1.60]**
Bloating		◦							0.44 [−0.06, 0.95]	**0.57 [0.06,1.09]**
Fullness				◦					0.51 [−0.01, 1.02]	0.46 [−0.06, 0.97]
Epigastric Pain		◦			•				**0.82 [0.10, 1.53]**	**1.33 [0.55, 2.09]**
Epigastric Burn		◦					•	•	**1.23 [0.34, 2.08]**	**1.11 [0.26, 1.93]**
Cardiac Pain		◦							**0.76 [0.23, 1.27]**	**0.74 [0.21, 1.26]**
Cardiac Burn		◦			•			•	**1.63 [0.46, 2.75]**	**1.74 [0.53, 2.89]**

[a]Cohen's *d* was used here as a metric to estimate the magnitude and relative significance of the symptom improvement (i.e., reduction in absolute GCSI symptom scores) to be expected when GES is tuned to produce particular types of vagal responses (shown in each row next to the symptom names). A Cohen's *d* value greater than 0.8 represents a large treatment effect (while greater than 1.2 is considered to be a very large effect and greater than 2 an enormous effect) (Cohen, 1962; Cohen, 1988). Data are reported as Cohen's *d* estimate [95% confidence interval]. Cohen's *d* values that indicate a significant effect of fiber recruitment on less severe or frequent symptoms are in **bold** font. N = 66 subjects included in this analysis.